



FRAGILITY CURVES FOR A THREE-STOREY REINFORCED CONCRETE TEST STRUCTURE OF THE INTERNATIONAL BENCHMARK SMART 2013

S. Rajan⁽¹⁾, C. Butenweg⁽²⁾, L.A. Dalguer⁽³⁾, J. H. An⁽⁴⁾, P. Renault⁽⁵⁾, S. Klinkel⁽⁶⁾

⁽¹⁾ Research Assistant, RWTH-Aachen University, rajan@lbb.rwth-aachen.de

⁽²⁾ Professor, SDA-engineering GmbH, butenweg@sda-engineering.de

⁽³⁾ Structural Engineer, swissnuclear, luis.dalguer@swissnuclear.ch

⁽⁴⁾ Structural Engineer, GERB Engineering GmbH, an.junghyun80@gmail.com

⁽⁵⁾ Managing Director, swissnuclear, philippe.renault@swissnuclear.ch

⁽⁶⁾ Professor, RWTH-Aachen University, klinkel@lbb.rwth-aachen.de

Abstract

Within the framework of the international benchmark project SMART 2013 (www.smart2013.eu) the robustness of the half part of a typical simplified electrical nuclear reinforced concrete building (1/4 scale) was investigated under various seismic loading conditions. Most of Nuclear Installations in Europe are located in low seismicity area. The hazard in these zones predicts moderate to large events that are required for the input of risk assessment of critical structures such as nuclear power plants. But there is lack of observed data for such events at the site of study. Therefore, a database of 50 sets of synthetic accelerograms, each set composed by two horizontal components, were applied as seismic excitation to the reinforced concrete structure. These synthetics are compatible with an earthquake of magnitude $M = 6.5$ at distance 9 km from the source.

This paper presents the fragility analysis of the SMART 2013 test structure. The seismic response of the structure has been calculated using the ABAQUS solver. The structure is asymmetric and has been modeled with the three dimensional finite-element method that consists of conventional shell and beam elements. Concrete damaged plasticity model of ABAQUS has been used for the concrete and a bilinear-elastic perfectly-plastic model for the steel. The structural response is calculated by the full dynamic time history and the pushover analysis. The results of these two calculations are compared and used for the derivation of fragility curves with PGA as seismic indicator. The results from the dynamic analysis indicate that, due to the asymmetrical characteristic of the structure, there is a significant difference in the prediction of probability of damage in X and Y direction of the structure for linear and nonlinear structural behavior. Moreover, the comparison of the lognormal standard deviation shows that nonlinear dynamic analysis gives more accurate results compared to that of the pushover analysis. However, the computational time is considerably reduced in the case of pushover analysis.

Keywords: SMART, fragility, RC Structure, nonlinear analysis, pushover



1. Introduction

Reinforced concrete (RC) is widely used for the construction of all type of structures, such as buildings, bridges or any other infrastructure. Conventional RC structures usually consist of moment resisting frames. Here a non-conventional heavy structure (1/4 reduced scale) from a nuclear power plant (NPP) with reinforced concrete walls is considered for the development of fragility curves to evaluate the vulnerability of the structure under seismic excitation.

The methodology for the development of fragility curves has been proposed by various authors and has been applied by several others in the literature. The major difference in the methods proposed by various authors are in the consideration of the uncertain parameters, uncertainty in seismic loading, selection of seismic indicators and computational method. The fragility analysis for the conventional RC frames can be found in several literatures. For example Dumova-Javanska [1] proposed a method to consider Modified Mercalli Intensity Scale(MMI) as a seismic intensity indicator instead of the commonly used seismic indicators Peak Ground Acceleration (PGA); Ellingwood et al [2] determined the fragility using spectral acceleration as the seismic indicator and considering epistemic uncertainties of the material parameters; Gardoni et al [3] considered different type of epistemic uncertainty and the fragility curves were based on the demand variables; Kinali and Ellingwood [4] carried out the fragility analysis for steel frames; Park et al [5] proposed a method to combine the deformation with the absorbed energy of the system and to plot the fragility with characteristic intensity and damage index which depicts the structural damage; Buratti et al [6] used response surface to plot the fragility curves of the reinforced frame. The fragility curves for the bridges has been analyzed, among others, by Shinozuka et al [7], Mackie et al [8] and Mander et al [9]. The fragility analysis of nuclear power plants can e.g. be found in Kennedy and Ravindra [10] and for the concrete gravity dams in Teckie and Ellingwood [11]. The development of fragility curves in all these cases considers the uncertainty and randomness of the structural parameters and/or the loading.

The selection of the numerical methods for the fragility analysis plays an important role for the accuracy and computational time, as such, it should be given ample importance. According to Shinozuka et al [7], the most reliable analytical approach for the development of fragility curves is using nonlinear time-history analysis. However, the physical interpretation of the results is sophisticated. Moreover, the computational time is also very high depending on the nonlinear properties, while in simplified methods, such as pushover analysis, the computational time is considerably reduced. In this paper, we develop fragility curves of the reinforced concrete test structure, respectively, from the results of the nonlinear time-history and nonlinear static pushover methods. For this purpose, a test structure from the SMART 2013 project [12] is considered, in which laboratory experiments on a shaking table were carried out on a reduced scale (1/4) model of the half part of a typical simplified electrical nuclear RC building. The technical specification of the SMART 2013 international benchmark which includes the general description of the benchmark and the mock-up, seismic inputs, material parameters, recommendation for the structural analysis and fragility curve calculations can be found in Richard and Chaudat [13]. The software package ABAQUS is used to evaluate the structure using the mentioned two methods (time history and pushover).

For verification (validation) purpose of the numerical methods, initially the response of the structure under seismic excitation corresponding to recorded ground motion of the Northridge earthquake and one of its after-shocks is evaluated using nonlinear dynamic analysis (time-history) as well as pushover analysis. Then, the results are compared with the experimental data from SMART 2013 [12]. Subsequently, fragility curves are developed, respectively for the time-history and pushover analysis, using a database of 50 sets of synthetic accelerograms, each set composed of two horizontal components. These synthetic accelerograms are compatible with an earthquake of magnitude $M=6.5$ at a distance 9 km from the source.

2. Numerical modeling and analysis methods

The test structure is a three-story reinforced concrete structure, with a trapezoidal geometry. A picture, a plan view and the Finite Element (FE) model of the structure are shown in Fig. 1.

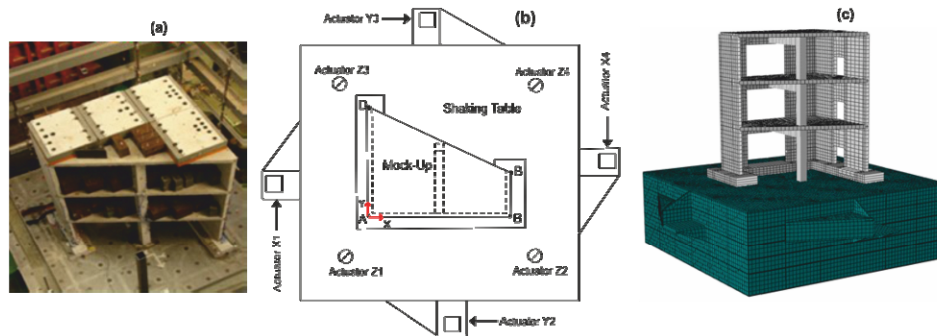


Fig. 1 – RC structure (a) photo [19] (b) Plan view with shaking table (c) Numerical model with shaking table

The numerical modeling of the test structure (mock-up) is developed using the finite element software package ABAQUS. We improved (refined) the model presented by Dalguer et al [14, 15], in which the development of the numerical models is done by testing the boundary conditions and constitutive laws of the RC structure and its local specimens under quasi-static excitation with and without reinforcement. Further details regarding the local specimen test is not included here to limit the scope of the paper and can be found in Dalguer et al [14].

All structural elements of the mock-up are included in the numerical model with the geometry and material characteristics provided by the benchmark project organizers. The RC columns and beams are modeled by Timoshenko (shear flexible) 3D beam element of type B31 with linear interpolation. All RC walls, slabs and the foundation beam are modeled with triangular (type S3R) and quadrilateral (type S4R) conventional large-strain shell elements. Previous experience from the benchmark suggest that the shaking table cannot be ignored because there is a certain degree of interaction. Therefore the shaking table is assumed as a semi-rigid block of steel and modeled with shell elements (type S3R and S4R). Composite nature of reinforced concrete due to the presence of concrete and steel, makes it complex with a combination of different mechanical properties and strong material nonlinearity. For the concrete, there are several constitutive models proposed in the literature (eg. Kaar et al [15], Lee and Fenves [17], Lubliner et al [18]). Here, the concrete damage plasticity (CDP) model of ABAQUS is used. The CDP is a modification of the Drucker-Prager plasticity model. Reinforcing steel exhibits linear elasticity up to a certain stress, after which it changes to a nonlinear-inelastic behavior, usually referred to as plasticity. This plastic behavior is represented by a bilinear elastic-perfectly-plastic model. Calibration of the model is done by evaluating the linear elastic characterization of the numerical model of the structure by performing modal analysis.

2.1 Modal analysis

Modal analysis is used to calibrate the numerical model by comparing the calculated natural frequencies with that measured in the experimental data. The eigenvalues extraction is done by using the Lanczos eigensolver and Rayleigh damping of 5% is applied. Three different boundary conditions were considered: Case 1, the mock-up is fixed at the foundation level and is not loaded with additional masses: Case 2, the mock-up is fixed at the foundation level and is loaded with additional masses (as shown in Fig. 1a, the mock-up was loaded with self-weight and additional loads). To simplify the numerical model, the additional masses are modeled as non-structural masses with mass proportional distribution on each slab. In Case 3, the shaking table along with the structure and additional masses are modeled and anchorage points between the actuators and the shaking table is considered to be fixed. These elements have been calibrated in order to fit the first two fundamental frequencies



of the structure. Rayleigh numerical damping is introduced in the nonlinear material model with a value of 5.0% on the first natural frequency (5.99 Hz) and 5.0% on the third one (19.84 Hz).

Table 1 – Natural frequencies of the structure [Hz]

Mode	Experiment	Case1	Case2	Case3
1	6.28	20.68	8.70	5.99
2	7.86	36.07	15.64	9.28
3	16.50	64.29	29.95	19.84

The first three natural frequencies of the three cases and the ones observed in the experiments are listed in Table 1. Case 3 results are more consistent with the experiment. The vibration modes are complex as shown in Figure 2 that correspond to the case 3. The first and second modes are dominated by translational vibration in X and Y direction and a rotation of the structural system, originated from the unsymmetrical geometry configuration and stiffness difference of the mock-up. In the third mode shape the mock-up responds with torsional vibration.

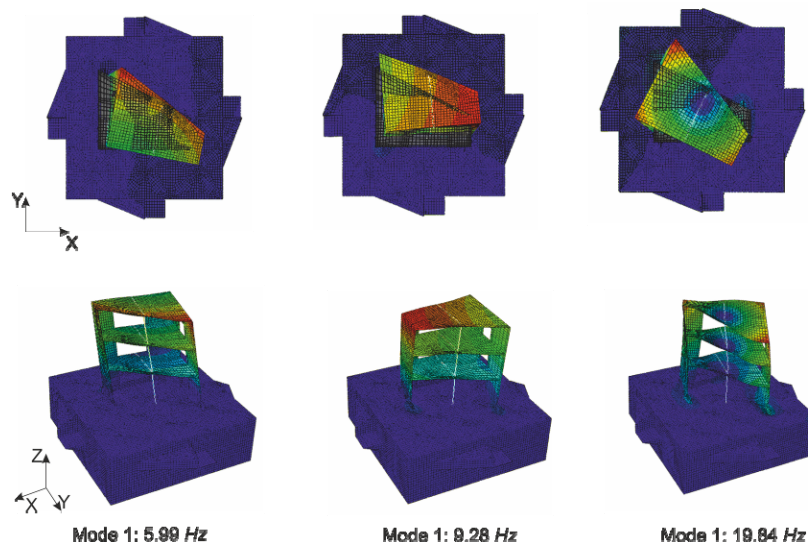


Fig. 2 – Mode shapes corresponding to Case 3 of the test structure with shaking table

2.2 Numerical methods

As stated earlier, nonlinear time-history analysis is the most reliable approach to evaluate the structural response of RC structure. Due to higher computational effort and complex nature of the results, time-history analysis are not always preferred. Alternatives include pushover analysis, where the nonlinear structural behavior during seismic excitation are computed using static analysis. Here, nonlinear dynamic analysis and pushover analysis are carried out on the same numerical model.

2.2.1 Dynamic nonlinear time history analyses

Dynamic nonlinear time history analyses, also called transient dynamic analyses, are performed using the ABAQUS implicit solver (which use the HHT time integration) subjected to a given set of ground motions. The highly nonlinear constitutive model for concrete provided by ABAQUS, the so called concrete damage plasticity (CDP), is used. The solver successfully finds solutions for all the input ground motions including the strong



shaking of the main shock from Northridge earthquake. The test was performed for the linear and nonlinear analysis. In the case of non-linear analyses the peak ground acceleration ranging from 0.2g to 1g is considered. Plastic strain under the strong shaking of PGA of 1g is concentrated on the walls at the ground level and at the intersection of the walls at the foundation level as shown in Figure 3. A small amount of plastic strain is observed at the window's corner of each floor.

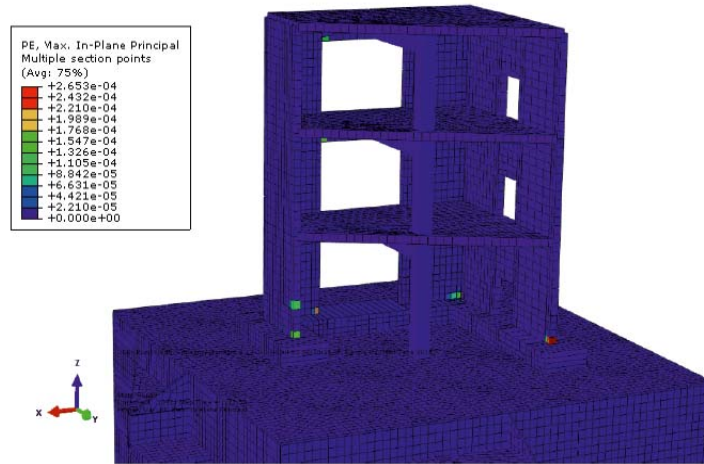


Fig. 3 – Plastic strain distribution of nonlinear dynamic response of the structure under PGA of 1 g

2.2.2 Pushover analysis

For comparison purposes and for the benefit of a reduced computational time, a nonlinear static pushover analysis is developed to determine the behavior of the structure. ABAQUS explicit solver is also used for this analysis. The structure is subjected to monotonically increasing lateral forces with a height-wise and mass-wise distribution until the target displacement is reached. Then, the capacity curves are plotted based on the force-displacement relationship. However, the application of nonlinear pushover analysis to irregular buildings with torsional modes is quite complex and requires the consideration of all relevant modes of vibrations. A modal pushover analysis method was suggested by Chopra and Goel [19], a modified version of this method named multi-modal pushover analysis [20] is employed here. The analysis is carried out considering the first three eigenmodes and their combinations by means of equivalent static forces applied to the reinforced concrete structure. The resulting nonlinear load displacement curve obtained from the pushover analyses are shown in Fig. 4a. The response spectrum corresponding to the time history is shown in Fig. 4b. The load displacement curve is superposed to the curve spectral acceleration (S_a) vs. spectral displacement (S_d) to determine the so called “Performance Point” as shown in Fig. 4c

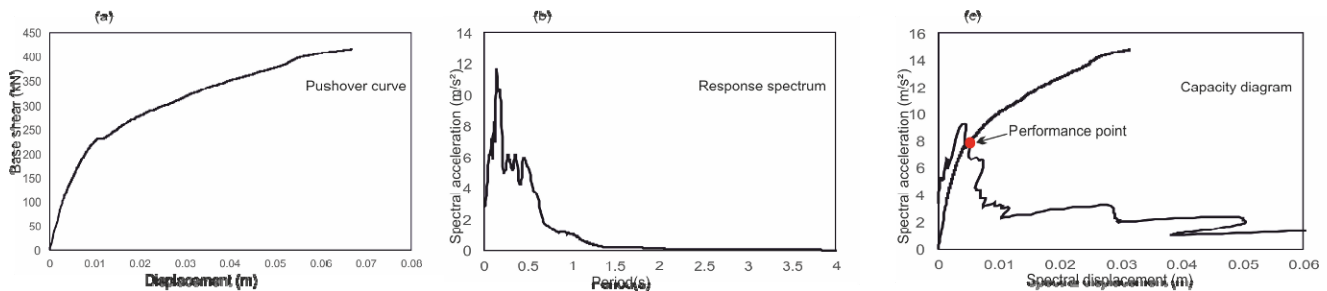


Fig. 4 – (a) Pushover curve (b) Site response spectra (c) Capacity diagram



3. Validation

The calibrated model (developed in Section 2.1) with the shaking table is composed of conventional shell and beam elements with a total of 60517 elements and 52793 nodes. This model is then validated for the linear range using lower intensity ground motions (PGA of 0.10g) and for the nonlinear behavior using higher intensity ground motions (PGA of 0.2g to 1g). The numerical models and methods are validated by comparing with the experimental results from SMART2013.

3.1 Validation of the time-history analysis

The numerical model behavior is validated using the measured experimental response. The displacement and acceleration response at several points (A, B, C, D as shown in Fig. 1) of the structure are compared with that of the experiment. For instance, Figure 5 shows a typical example that compares floor-displacement and acceleration time history at point D at the top floor of the structural response under the seismic excitation identified by the ground motions #07, #09 and #19, respectively with PGA 0.1g, 0.2g and 1g.

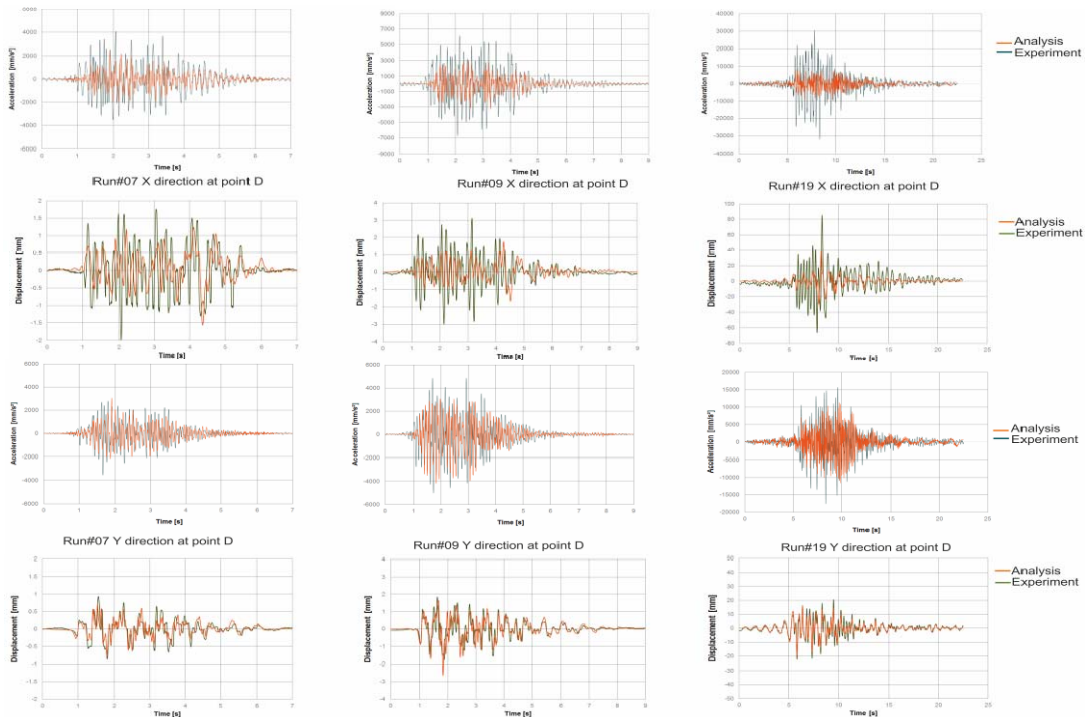


Fig. 5 – Comparison of the acceleration and displacement response of run #07 (PGA 0.1g) #09 (PGA 0.2g) and #19 (PGA of 1g) with experiment

As shown in Fig. 5, the comparison with the experiment results in the linear range (run #07) of the acceleration and displacement response closely match in both X and Y directions. For the nonlinear case with lower PGA (run #09), the numerical results are comparable with that of the experiment. But for higher PGA (run #19) the displacement and acceleration amplitudes are underestimated. These deviations are maybe due to the unrealistic connection with the test structure and very stiff shaking table. The assumption of fixed connection between the shaking table and the test structure is made in the numerical analysis. However, in the actual experiment the connection is established using the anchor bolts. The interaction between test structure and shaking table needs further investigation. As simplification, the numerical model, used for the fragility analysis, has springs and dashpots to substitute the shaking table. The behavior in Y direction is consistent with that of the experiment in all cases. Validation of the pushover analysis method is not done since a one to one comparison with experiment was not feasible. Therefore, for the pushover case the same numerical model with spring and dashpot boundary conditions is used for the fragility analysis.



4. Development of fragility curves

A reliable assessment of seismic vulnerability of buildings depends mainly on the criteria to define the level of damage, the threshold for failure criteria and the seismic intensity measure. Due to the intrinsic uncertainty (usually very large) to define those parameters, the analysis is performed in a probabilistic sense. This results in the development of the so called fragility curves, which are the conditional probability to define a specific damage level for a given level of seismic intensity. A thorough compilation of development of fragility curves can be seen in Calvi et al [21]. In this paper we followed the recommendations of SMART 2013 project [13] for the calculation of fragility curves. In order to consider a realistic RC structural behavior, the numerical model includes equivalent foundation to represent the soil-structure interaction (SSI) effect. This is done introducing springs and dashpots, so that features of SSI, such as swaying, pumping and rocking motion can be represented. The stiffness and damping to be considered for spring and dashpots were given in the SMART 2013 technical specifications [13].

4.1 Method description and damage indicator

The description of the procedure is the same as described in Dalguer et al [15] that follows the SMART project specifications [13]. The damage indicator is defined by the maximum inter-story drift at point D (in the X and Y directions). Three levels of damage are considered: Light damage (drift = $h/400$), controlled damage (drift = $h/200$), and extended damage (drift = $h/100$), where h is the story height. We used PGA as the seismic indicator.

A lognormal fragility model is chosen, therefore the fragility curve is entirely defined by two parameters, which are the median capacity A_m and the lognormal standard deviation β . Details of the methodology for determining fragility curves followed in this paper, and recommended by the SMART project, is given in the appendix 3 of the technical specifications of the project [13]. The fragility curve is generally modeled using a lognormal cumulative distribution function, a choice supported by studies in the past in different fields for e.g. Ellingwood [22], Singhal and Kiremidjian [23], Shinozuka et al [24]. Therefore, the fragility curve is mathematically described as given in Eq. 1,

$$P_f(\theta) = \Phi\left(\frac{\ln(\theta / A_m)}{\beta}\right) \quad (1)$$

Where Φ is the standard normal probability distribution function, θ is the seismic intensity (PHA in this study), A_m is the median capacity expressed in terms of θ , β is the lognormal standard deviation. The median capacity and lognormal standard deviation can be determined either by regression analysis or maximum likelihood method [24],[25]. We use a linear regression to predict damage for a given intensity. The obtained inter-story drift from both nonlinear pushover analyses and nonlinear dynamic analyses of the numerical model is accounted here. The empirical relationship obtained from these analyses is a linear equation as given by Eq. 2.

$$\ln(D) = a + b \ln \theta \quad (2)$$

Here, a and b are the coefficients from the regression analysis. The value of A_m is then computed using Eq. 3, D_d is the critical threshold of damage indicator.

$$\ln(A_m) = \frac{\ln(D_d) - a}{b} \quad (3)$$

The lognormal standard deviation β is computed from the dispersion of data in Eq.2 and is given by the Eq. 4.

$$\beta^2 = \frac{1}{N} \sum_{i=1}^N [\ln(D_i) - \ln(D)]^2 \quad (4)$$



4.2 Fragility curves derived using dynamic analyses

The fragility curves obtained using linear and nonlinear dynamic analyses are shown in the Fig. 6. The drift predictor is calculated using the linear regression as shown on the left in the Fig. 6. The predictor line in linear and nonlinear case are different for X and Y direction. In the X direction the linear case predicts larger values than the nonlinear case. In Y direction it is vice versa. This is maybe due to higher stiffness in the Y direction which is underestimated in the non-linear case. The linear analysis gives a more conservative prediction in X direction, whereas in Y direction nonlinear analysis gives a conservative prediction.

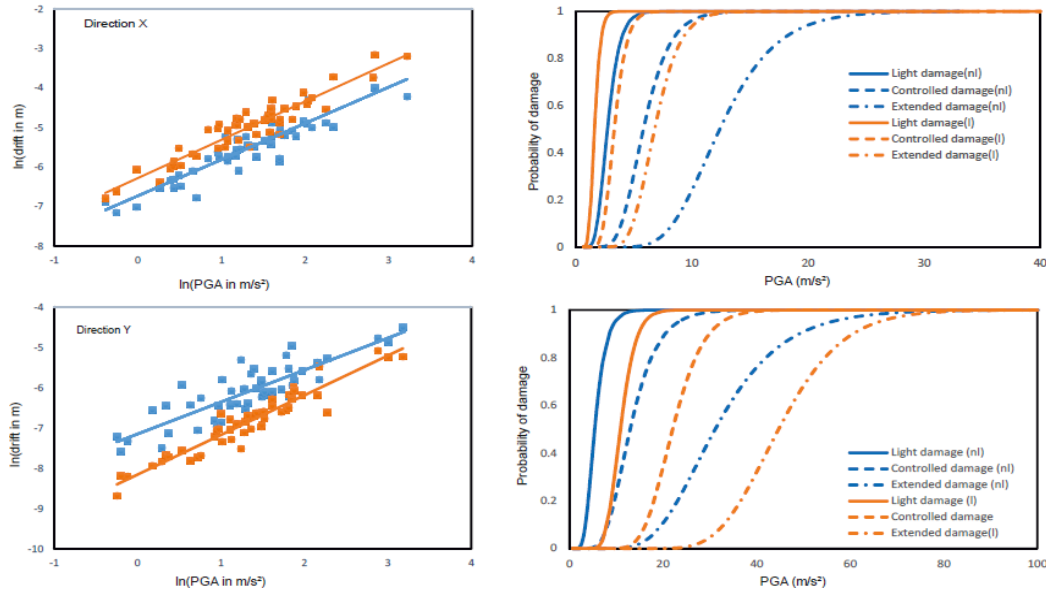


Fig. 6 – [left] Linear regression, [right] Comparison of linear and nonlinear fragility curves for PGA

4.2 Fragility curves using pushover analysis

The calculation of the fragility curves using the data from pushover analysis is performed in the same way as described above. The drift predictor is estimated from linear regression of the database composed by drift and seismic intensity (PGA) in logarithm quantities. The drift in the pushover response indicates the performance point corresponding to each response spectrum which is obtained as shown in Fig. 4. All possible combination of the first three modes have been investigated, but just the combination for the maximum displacement in X direction is presented here. The performance point was not achieved in the numerical analysis for PGA over 0.9g and a 5% damped spectrum. The main reason of it could be that at higher PGA the nonlinear behavior of the structure is well pronounced, so the model is not efficiently representing the high nonlinearity. Furthermore, the energy dissipation of the structure during higher intensity earthquake is higher, which is not reflected in the 5% damped elastic spectra. We suggest to use a 10% or 15% damped spectrum for a higher intensity earthquake (PGA over 0.9g). However this needs further investigations. The fragility curves of the nonlinear static (pushover) analysis for a combination of 1st and the 3rd mode in X direction is shown in the Fig. 7(a).

A comparison of the fragility curves of the nonlinear dynamic and pushover analysis in X direction is shown in the Fig. 7(b), the prediction of the damage behavior is more conservative for nonlinear dynamic analysis in the case of light and controlled damages. Whereas in the case of extended damage, the fragility curves using the pushover analysis tend to be more conservative. More accurate results could have been achieved using pushover analysis with the consideration of nonlinear behavior/damping. However, further investigations are



required in this context. A comparison of the median capacity and lognormal standard deviation is given in Table 2.

Table 2 – Mean value of median capacity A_m and lognormal standard deviation β in X direction

	Median capacity A_m			β
	Light damage	Controlled damage	Extended damage	
SMART 2013	2.82	5.67	12.06	0.50
Nonlinear dynamic	2.74	5.83	12.41	0.31
Pushover	4.23	6.81	10.97	0.46

The lowest standard deviation is obtained in the case of nonlinear dynamic analysis, suggesting that this method is more accurate when the maximum drift is considered as failure criteria. The standard deviation obtained in the experiment is comparatively higher than the numerical cases, whereas the median capacity is approximately the same. The lognormal standard deviation observed from the pushover analysis is also comparatively higher, this might be due to the fact that the consideration of the 5% damped spectra is not sufficient in the case of higher PGA. Further investigation is solicited in this regards.

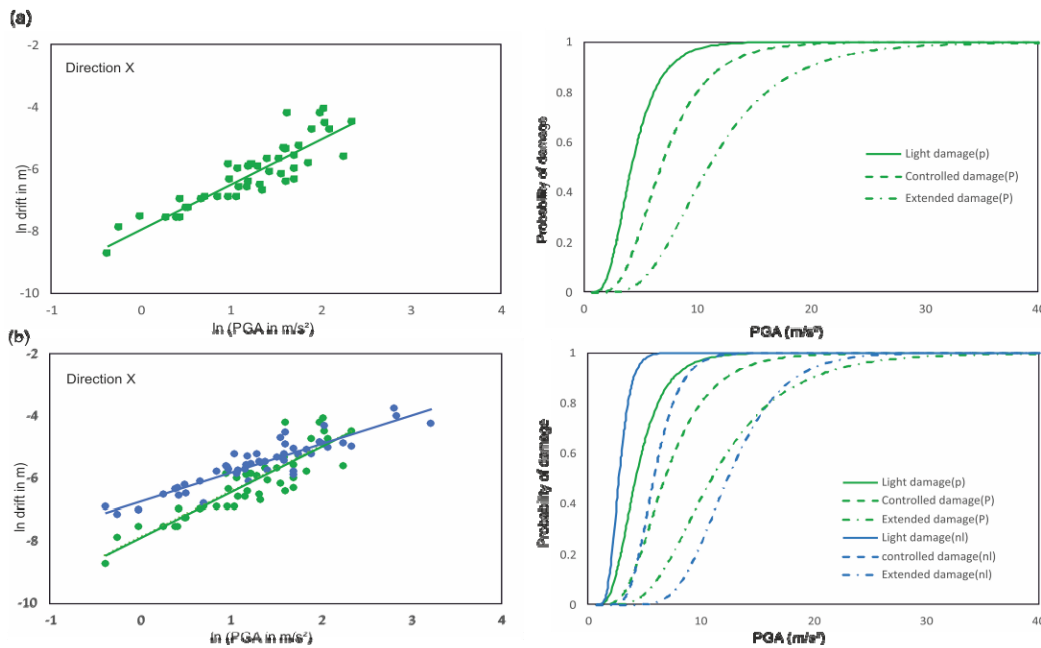


Fig. 7 – [a] Linear regression and fragility curves for pushover analysis, [b] Comparison of fragility curves for nonlinear dynamic analysis and pushover analysis

5. Discussions and Conclusions

Fragility curves have been developed for the SMART 2013 test structure assuming PGA as seismic indicator for 50 sets of synthetic ground motions corresponding to a magnitude $M=6.5$ at a distance of 9 km from the source. The validation of the numerical model is done using the results from the SMART 2013 benchmark. The behavior of the numerical model for higher PGA in X direction shows discrepancies with the experiments. This is due to the assumption of the connection between the test structure and shaking table considered as semi-rigid. Appar-



ently these assumptions did not represent the actual bolted connection. The fragility curves have been derived for the test structure assuming that the structure is on a soil foundation. With the aim to represent the soil-structure interaction effects, the foundation is modeled with a spring-dashpot system. Two methods were selected for the analysis of the structure; nonlinear dynamic analysis and nonlinear static pushover analysis.

In the dynamic analysis, a comparison is done for the linear and nonlinear response of the structure. Due to the asymmetrical characteristic of the structure, there is a significant difference in the prediction of probability of damage in X and Y direction of the structure. The derived fragility curve shows that in X direction the linear dynamic analysis gives a more conservative value of the capacity compared to the nonlinear analysis. Y direction the results are vice versa. The comparison of the lognormal standard deviation shows that nonlinear dynamic analysis gives more accurate results compared to that of the pushover analysis. However, the computational effort is considerably reduced in the case of pushover analysis. Further investigations are required for the pushover analysis in order to consider the nonlinear effects resulted from the loading of high intensity values, such as those from large earthquakes.

6 Acknowledgement

We would like to thank the organizers of SMART2013 for the opportunity to participate in the benchmark project and swissnuclear for the financial support to carry out this work. The first author also gratefully acknowledge the financial support from BMWi (Bundesministerium für Wirtschaft und Energie) for the project number 1501503.

7. References

- [1] Dumova-Jovanoska, E. (2000). Fragility curves for reinforced concrete structures in Skopje (Macedonia) region. *Soil Dynamics and Earthquake Engineering*, 19(6), 455-466.
- [2] Ellingwood, B. R., Celik, O. C., & Kinali, K. (2007). Fragility assessment of building structural systems in Mid-America. *Earthquake Engineering & Structural Dynamics*, 36(13), 1935-1952.
- [3] Gardoni, P., Der Kiureghian, A., & Mosalam, K. M. (2002). Probabilistic capacity models and fragility estimates for reinforced concrete columns based on experimental observations. *Journal of Engineering Mechanics*, 128(10), 1024-1038.
- [4] Kinali, K., & Ellingwood, B. R. (2007). Seismic fragility assessment of steel frames for consequence-based engineering: A case study for Memphis, TN. *Engineering structures*, 29(6), 1115-1127.
- [5] Park, Y. J., Ang, A. H. S., & Wen, Y. K. (1985). Seismic damage analysis of reinforced concrete buildings. *Journal of Structural Engineering*, 111(4), 740-757.
- [6] Buratti, N., Ferracuti, B., & Savoia, M. (2010). Response surface with random factors for seismic fragility of reinforced concrete frames. *Structural Safety*, 32(1), 42-51.
- [7] Shinozuka, M., Feng, M. Q., Kim, H. K., & Kim, S. H. (2000). Nonlinear static procedure for fragility curve development. *Journal of engineering mechanics*, 126(12), 1287-1295.
- [8] Mackie, K., & Stojadinović, B. (2003). *Seismic demands for performance-based design of bridges*. Pacific Earthquake Engineering Research Center.
- [9] Mander, J. B. (1999). Fragility curve development for assessing the seismic vulnerability of highway bridges. *Research Progress and*, 89.
- [10] Kennedy, R. P., & Ravindra, M. K. (1984). Seismic fragilities for nuclear power plant risk studies. *Nuclear Engineering and Design*, 79(1), 47-68.
- [11] Tekie, P. B., & Ellingwood, B. R. (2003). Seismic fragility assessment of concrete gravity dams. *Earthquake engineering & structural dynamics*, 32(14), 2221-2240.
- [12] <http://www.smart2013.eu/>



- [13] Richard, B., & Chaudat, T. (2014). Presentation of the SMART 2013 International Benchmark. *CEA/DEN Technical Report. DEN/DANS/DM2S/SEMT/EMSI/ST/12-017/H*.
- [14] Dalguer, L.A.; S. Churilov, C. Butenweg, Ph. Renault and A-J. Hyun (2014), Dynamic Analysis of a Reinforced Concrete Electrical Nuclear Building of SMART 2013 Project Subjected to Earthquake Excitation using ABAQUS, *Proceedings of the SMART2014 Workshop*, Paris, France, November 25-27, 2014.
- [15] Dalguer, L. A., Ph. Renault; S. Churilov, C. Butenweg (2015), Evaluation of Fragility Curves for a three-Storey Reinforced Concrete Mock-up of SMART 2013 project. *Transaction, 23th International Conference on Structural Mechanics in Reactor Technology (SMiRT-23), Division V*, Manchester, United Kingdom, August 10-14, 2015.
- [16] Kaar, P.H., Hanson, N. W. and Capell, H.T. (1978). “Stress-strain curves and stress block coefficients for high strength concrete”, *ACI Special Publication*
- [17] Lee, J., Fenves G.L “Plastic-damage model for cyclic loading of concrete structures”, *J. Engineering Mechanics*, 124 (10), 892-900.
- [18] Lubliner, J., Oliver J., Oller S. and Onate E. (1989) “A plastic-damage model for concrete”, *International Journal of Solids and Structures*, 25, 299-329.
- [19] Chopra, A. K., & Goel, R. K. (2001). A modal pushover analysis procedure to estimate seismic demands for buildings: Theory and preliminary evaluation. *Civil and Environmental Engineering*, 55.
- [20] Norda, H. (2013). *Beitrag zum statischen nichtlinearen Erdbebennachweis von unbewehrten Mauerwerksbauten unter Berücksichtigung einer und höherer Modalformen*. Lehrstuhl für Baustatik und Baudynamik.
- [21] Calvi, G. M., Pinho, R., Magenes, G., Bommer, J. J., Restrepo-Vélez, L. F., & Crowley, H. (2006). Development of seismic vulnerability assessment methodologies over the past 30 years. *ISET journal of Earthquake Technology*, 43(3), 75-104.
- [22] Ellingwood, B. (1990). Validation studies of seismic PRAs. *Nuclear Engineering and Design*, 123(2-3), 189-196.
- [23] Singhal, A., & Kiremidjian, A. S. (1996). Method for probabilistic evaluation of seismic structural damage. *Journal of Structural Engineering*, 122(12), 1459-1467.
- [24] Shinozuka, M., Feng, M. Q., Lee, J., & Naganuma, T. (2000). Statistical analysis of fragility curves. *Journal of Engineering Mechanics*, 126(12), 1224-1231.
- [25] Zentner, I. (2010). Numerical computation of fragility curves for NPP equipment. *Nuclear Engineering and Design*, 240(6), 1614-1621.